

Duality Between the Webs of Heterotic and Type II Vacua

PHILIP CANDELAS¹ AND ANAMARÍA FONT²

*Theory Group
Department of Physics
University of Texas
Austin, TX 78712, USA*

ABSTRACT

We discuss how transitions in the space of heterotic $K3 \times T^2$ compactifications are mapped by duality into transitions in the space of Type II compactifications on Calabi–Yau manifolds. We observe that perturbative symmetry restoration, as well as non-perturbative processes such as changes in the number of tensor multiplets, have at least in some cases a simple description in terms of the reflexive polyhedra of the Calabi–Yau manifolds.

¹ candelas@physics.utexas.edu.

² afont@dino.conicit.ve. On sabbatical leave from Departamento de Física, Facultad de Ciencias, Universidad Central de Venezuela.

1. Introduction

In this note we explore four-dimensional, $N=2$ string vacua in connection with the conjectured duality [1,2] between $(0,4)$ compactifications of the $E_8 \times E_8$ heterotic string on the manifold $K3 \times T^2$ and the type IIA string compactified on a Calabi-Yau manifold. This duality has been the subject of several articles in the recent literature [3-11]. Schematically we may write

$$\text{Het}_{E_8 \times E_8}[K3 \times T^2, \mathcal{V}] \simeq \text{IIA}[\mathcal{M}]$$

where \mathcal{V} denotes the bundle (more properly a sheaf) corresponding to the background gauge field and $\mathcal{M} = \mathcal{M}_{\mathcal{V}}$ a Calabi-Yau manifold that depends on \mathcal{V} . This duality induces a correspondence

$$\mathcal{V} \leftrightarrow \mathcal{M}_{\mathcal{V}}$$

between vector bundles on $K3 \times T^2$ and certain (perhaps all) Calabi-Yau manifolds, though a special role is played by manifolds that are $K3$ -fibrations [3,4,9]. The evidence supporting this correspondence is based on the identification of certain dual pairs $(\mathcal{V}, \mathcal{M}_{\mathcal{V}})$ through a computation of Hodge numbers and, very compellingly, on detailed comparison of the structure of the moduli-spaces of \mathcal{V} and $\mathcal{M}_{\mathcal{V}}$ for candidate dual pairs previously identified on the basis of their Hodge numbers[1,6,7,12,13].

Two observations concerning this duality are the subject of the present article: that a great many Calabi-Yau manifolds are known in terms of toric data[14-17] and the correspondence, pointed out by Batyrev, between Calabi-Yau manifolds and reflexive polyhedra [18]. Proceeding loosely: we have a correspondence between reflexive polyhedra, Δ , and Calabi-Yau manifolds \mathcal{M}_{Δ} . Combining this with the correspondence between vector bundles \mathcal{V} and Calabi-Yau manifolds gives a correspondence between vector bundles on $K3 \times T^2$ and reflexive polyhedra $\mathcal{V} = \mathcal{V}_{\Delta}$. It is known also that the moduli spaces of Calabi-Yau manifolds form a web in which continuous transitions between different Calabi-Yau manifolds (phases) occur due to the shrinking to zero of certain homology two cycles and three cycles as the parameters of the manifold are varied[19-22]. Indeed it seems likely that all Calabi-Yau manifolds are connected by processes of this type[23-26]. The consistency and continuity of the string vacua associated with this process is assured by effects involving solitons that wrap the vanishing cycles and which become massless at the transition where the cycles vanish[27-30]. In virtue of duality this web structure must exist also on the heterotic side, though the physical picture is different. Indeed, the space

of heterotic vacua also forms a web in which different models are connected along branches parametrized by vacuum expectation values of scalars in vector and hypermultiplets that correspond to the parameters of \mathcal{V} . In virtue of the correspondence $\mathcal{V} \leftrightarrow \Delta$ there should be a dictionary that translates between the language of reflexive polyhedra and that of heterotic dynamics, including the non-perturbative effects uncovered by new insight into string phenomena [31-33]. A first step towards finding such dictionary was taken in ref. [8] where it was noticed that un-Higgsing of $SU(r)$ groups in certain heterotic models matched into a chain of $K3$ fibrations. Subsequently, it was argued that the appearance of perturbative heterotic groups in these chains could be explained in the Calabi-Yau picture as well [10].

Motivated by the observations of [8], we point out that corresponding to a Higgsing chain of heterotic models, there is a chain of Calabi-Yau manifolds with a simple structure revealed by their description in terms of reflexive polyhedra. These manifolds are $K3$ fibrations. Indeed the four-dimensional polyhedron contains the polyhedron of the $K3$ in a simple way and it is this nesting of polyhedra that motivates much of our analysis. The heterotic models of [8] basically correspond to $K3 \times T^2$ compactifications in which instanton numbers $(d_1, d_2) = (24, 0), (20, 4), (18, 6), (16, 8)$ and $(14, 10)$ are embedded in $E_8 \times E_8$ [34]. Maximally Higgsing the initial gauge group leads to models that can be identified with type II compactifications on known $K3$ fibrations [1,8,35]. Starting at these ‘anchor points’, we then study the type II description of un-Higgsing of different group factors. Recent results of ref. [35] allow us to consider other values of (d_1, d_2) . In some cases we find it necessary to include the effect of $D = 6$ extra tensor multiplets in the heterotic construction [33]. Reversing our strategy, we have also analyzed type II processes that arguably correspond to non-perturbative heterotic effects. The resulting type II pattern strongly suggests that these processes indeed have a non-perturbative interpretation in terms of transitions in which the number of tensor multiplets jumps by one and an instanton shrinks to zero.

This note is organized as follows. In section 2 we analyze $K3$ and $K3 \times T^2$ heterotic compactifications, including possible Higgsing patterns. Theories of this kind have been studied in recent related work [32,33,35-38]. In section 3 we consider various sequences of reflexive polyhedra and determine their relation to heterotic models. In section 4 we present our conclusions and list some open questions. An appendix contains figures of some of the polyhedra that we discuss.

2. Heterotic Chains

The starting point is a heterotic $E_8 \times E_8$ compactification on $K3$ with $SU(2)$ bundles with instanton numbers (d_1, d_2) such that $d_1 + d_2 = 24$. When both $d_i \geq 4$, the resulting group is the commutant of the instantons which is $E_7 \times E_7$ with massless hypermultiplets transforming as **56**s and/or singlets under each E_7 . Using the index theorem we find the hypermultiplet spectrum

$$\frac{1}{2}(d_1 - 4)(\mathbf{56}, \mathbf{1}) + \frac{1}{2}(d_2 - 4)(\mathbf{1}, \mathbf{56}) + 62(\mathbf{1}, \mathbf{1}) .$$

When $d_1 = 24, d_2 = 0$, the gauge group is $E_7 \times E_8$ and the massless hypermultiplets include

$$10(\mathbf{56}, \mathbf{1}) + 65(\mathbf{1}, \mathbf{1}) .$$

Without loss of generality we can take $12 \leq d_1 \leq 20$, unless $d_1 = 24$. We also find it convenient to define

$$k \stackrel{\text{def}}{=} \frac{d_1 - 12}{2} . \tag{2.1}$$

Since the **56** of E_7 is a pseudoreal representation, the d_i can be odd and k can be half-integer.

An initial heterotic model can be deformed by vevs of hypermultiplets thereby breaking the gauge group. Since $d_1 \geq 12$, the number of $(\mathbf{56}, \mathbf{1})$'s is such that the first E_7 can be completely broken. In particular, it can be broken through the chain

$$E_7 \rightarrow E_6 \rightarrow SO(10) \rightarrow SU(5) \rightarrow SU(4) \rightarrow SU(3) \rightarrow SU(2) \rightarrow SU(1) ,$$

where $SU(1)$ denotes the trivial group consisting of the identity only. On the other hand, the group arising from the second E_8 can only be broken to some terminal group $G_2^{(0)}$ that depends on k . For instance, $G_2^{(0)}(k) = E_8, E_7, E_6, SO(8)$ for $k = 6, 4, 3, 2$ and $G_2^{(0)}(k) = SU(1)$ for $k = 1, 0$.

The hypermultiplet content at every stage of breaking can of course be derived by group theory but it can also be found by imposing anomaly factorization conditions. Recall that the anomaly eight-form is given by

$$I_8 = \frac{1}{16(2\pi)^4} (\text{tr} R^2 - v_\alpha \text{tr} F_\alpha^2) (\text{tr} R^2 - \tilde{v}_\alpha \text{tr} F_\alpha^2) ,$$

where α runs over the various gauge factors. At Kac-Moody level one, the coefficients v_α are given by $v_\alpha = 2, 1, \frac{1}{3}, \frac{1}{6}, \frac{1}{30}$ for $\alpha = SU(N), SO(2N), E_6, E_7, E_8$ respectively [39]. The coefficients \tilde{v}_α depend on the hypermultiplet spectrum and can be determined from the form of the total anomaly [39]. For instance,

$$\begin{aligned} \tilde{v}_{E_8} &= -\frac{1}{5}, & \tilde{v}_{E_7} &= \frac{n_{56} - 4}{6}, & \tilde{v}_{E_6} &= \frac{n_{27} - 6}{6}, & \tilde{v}_{SO(10)} &= \frac{n_{16} - 4}{2}, \\ \tilde{v}_{SU(5)} &= n_{10} - 2, & \tilde{v}_{SU(4)} &= n_6 - 2, & \tilde{v}_{SU(3)} &= \frac{n_3 - 18}{6}, & \tilde{v}_{SU(2)} &= \frac{n_2 - 16}{6}, \end{aligned} \quad (2.2)$$

where n_R is the number of hypermultiplets in the R representation. In the case of $SO(10)$, $SU(5)$, and $SU(4)$, the number of fundamental representations is constrained to be $n_{10} = 2 + n_{16}$, $n_5 = 10 + 3n_{10}$ and $n_4 = 8 + 4n_6$ respectively. Finally, the total number of vector multiplets, n_V and hypermultiplets, n_H , satisfy the condition

$$n_H - n_V = 244 . \quad (2.3)$$

It is easy to check that (2.3) is satisfied in the initial (d_1, d_2) models described above.

In general, the gauge group is of the form $G = G_1 \times G_2$, with G_1 and G_2 coming from the first and second E_8 's. These groups are themselves products of simple factors. Notice that before Higgsing we have

$$\frac{\tilde{v}_1}{v_1} = k \quad , \quad \frac{\tilde{v}_2}{v_2} = -k , \quad (2.4)$$

where we have assumed $d_1 + d_2 = 24$, otherwise $\tilde{v}_2/v_2 = (d_2 - 12)/2$. After Higgsing, all non-Abelian factors contained in G_2 will satisfy $\tilde{v}_\alpha/v_\alpha = -k$. In particular, this implies that the $G_2^{(0)}(k)$ mentioned before are free of charged matter. Similarly, all non-Abelian factors contained in G_1 will satisfy $\tilde{v}_\alpha/v_\alpha = k$. For instance, if the first E_7 is broken to $SU(2)$, the number of doublets turns out to be

$$n_2 = 12k + 16 . \quad (2.5)$$

The number of $SU(2)$ singlets is obtained from (2.3). For example, if G is broken to $SU(2) \times G_2^{(0)}(k)$, we find

$$n_1 = 215 + \dim G_2^{(0)}(k) - 24k . \quad (2.6)$$

It is straightforward to repeat this sort of analysis for other breaking patterns.

Up to now we have focused on six-dimensional models. Upon further compactification on T^2 , the $N = 1$, $d = 6$ hyper and vector multiplets of G give rise to $N = 2$, $d = 4$ hyper and vector multiplets also of G , in numbers n_H and n_V that still must fulfill (2.3). The tensor multiplet produces an extra $U(1)$ vector multiplet associated to the dilaton and for generic 2-torus shape, there also appear two extra $U(1)$ vector multiplets corresponding to the torus that are usually denoted by T and U . Another new feature is the existence of a Coulomb branch parametrized by expectation values of the adjoint scalars in the $N = 2$ vector multiplets. At a generic point, excluding the graviphoton, the gauge group is $U(1)^{\text{rank } G+3}$ and the massless hypermultiplets include those n_{sing}^G fields originally neutral under G .

An $N = 2$, $D = 4$ heterotic model with the structure just described is potentially equivalent to a type IIA compactification on a Calabi–Yau manifold that is a $K3$ fibration and has

$$\begin{aligned} h_{11} &= \text{rank } G + 3 \\ h_{12} &= n_{sing}^G - 1 . \end{aligned} \tag{2.7}$$

In particular, maximal Higgsing of G to the matter-free $G_2^{(0)}(k)$ leads to

$$\begin{aligned} h_{11} &= \text{rank } G_2^{(0)}(k) + 3 \\ h_{12} &= 243 + \dim G_2^{(0)}(k) . \end{aligned} \tag{2.8}$$

Un-Higgsing an $SU(2)$ factor in G_1 then changes these numbers to

$$\begin{aligned} h_{11} &= \text{rank } G_2^{(0)}(k) + 4 \\ h_{12} &= 214 + \dim G_2^{(0)}(k) - 24k . \end{aligned} \tag{2.9}$$

Another interesting situation is the un-Higgsing of $SU(2) \times SU(2)$. In this case we find

$$\begin{aligned} h_{11} &= \text{rank } G_2^{(0)}(k) + 5 \\ h_{12} &= 185 + \dim G_2^{(0)}(k) - 40k . \end{aligned} \tag{2.10}$$

Similar results can be derived for other un-Higgsing patterns.

For $k = 6, 4, 3, 2, 1$, eqs. (2.8) yield Hodge numbers that match those of known $K3$ fibrations given by hypersurfaces of degree $12k + 12$ in $\mathbb{P}_4(1, 1, 2k, 4k + 4, 6k + 6)$ [1, 8, 35]. Remarkably enough, sequentially un-Higgsing $SU(r)$ factors ($r = 2, \dots, 4$) leads to Hodge numbers that also match into those of known $K3$ fibrations [8]. The chain of spaces thus obtained is shown in Table 2.1. Each element is then presumably equivalent to a heterotic $K3 \times T^2$ compactification in which the gauge group can be enhanced to

$$G = SU(r) \times G_2^{(0)}(k) \tag{2.11}$$

at special points in the heterotic moduli space. Indeed, it has been shown [10] that such enhanced groups can also appear in the conjectured type II dual compactification. Actually, since the toroidal $U(1)^2$ can be enhanced to $SU(3)$, there can be overall enhancement to a group contained in $G \times SU(3)$.

r	Calabi–Yau Manifold	$K3$
4	$\mathbb{P}_5^{(1,1,2k,2k+4,2k+6,2k+8)} [4k+8, 4k+12]$	$\mathbb{P}_4^{(1,k,k+2,k+3,k+4)} [2k+4, 2k+6]$
3	$\mathbb{P}_4^{(1,1,2k,2k+4,2k+6)} [6k+12]$	$\mathbb{P}_3^{(1,k,k+2,k+3)} [3k+6]$
2	$\mathbb{P}_4^{(1,1,2k,2k+4,4k+6)} [8k+12]$	$\mathbb{P}_3^{(1,k,k+2,2k+3)} [4k+6]$
1	$\mathbb{P}_4^{(1,1,2k,4k+4,6k+6)} [12k+12]$	$\mathbb{P}_3^{(1,k,2k+2,3k+3)} [6k+6]$

Table 2.1: The k 'th chain of hypersurfaces with enhanced group $SU(r) \times G_2^{(0)}(k)$, $k = 1, \dots, 6$.

The case $k = 5$ is special in that the chain of hypersurfaces do not in fact correspond to heterotic models of the type we have described since this would require $d_2 = 2 < 4$. Moreover, these hypersurfaces do not appear in the lists [14] of CY spaces in weighted \mathbb{P}_4 owing to the fact that the weights do not allow for transverse polynomials. This second objection is, however, easily dealt with. It is possible to give meaning to the manifolds of this chain in virtue of the correspondence between Calabi–Yau manifolds and reflexive polyhedra that is provided by the construction of Batyrev [18] in terms of reflexive polyhedra and it is therefore tempting to include this chain here. As for the first objection, we shall see in the next section, that the structure of the $K3$ polyhedra in the $k = 5$ chain is identical to that in the $k = 6$ chain. This strongly suggests that the terminal group is $G_2^{(0)}(5) = E_8$.

This proposal works if we modify the $N = 1$, $D = 6$ construction so as to include effects seen in the compactification of M -theory[40, 41, 32, 33] and F -theory [36,35]. More precisely we consider vacua with n_T tensor multiplets so that the condition $d_1 + d_2 = 24$ is replaced by

$$d_1 + d_2 + n_T - 1 = 24 . \tag{2.12}$$

We immediately see that $n_T = 3$ permits $d_1 = 22$, $d_2 = 0$. In this way we can have a $k = 5$ chain. Moreover, the initial gauge group $E_7 \times E_8$ can be completely broken to a matter-free E_8 .

The expressions for h_{11} and h_{12} must be modified since owing to the tensor multiplets, eq. (2.3) becomes [33]

$$n_H - n_V = 273 - 29n_T \quad (2.13)$$

and we must also take into account that upon further compactification on T^2 the n_T tensor multiplets give rise to n_T $U(1)$ vector multiplets. The effect is that eqs. (2.8) are now replaced by

$$\begin{aligned} h_{11} &= \text{rank } G_2^{(0)}(k) + n_T + 2 \\ h_{12} &= 272 + \dim G_2^{(0)}(k) - 29n_T . \end{aligned} \quad (2.14)$$

Eqs. (2.9) and (2.10) change accordingly. With $n_T = 3$ and $G_2^{(0)}(5) = E_8$ we recover the observed Hodge numbers of the $k = 5$ spaces.

For $k = 0$ we have a heterotic construction but this value does not admit of a simple interpretation in terms of the manifolds of Table 2.1. However, this interesting case can be analyzed following the approach of ref. [35]. Indeed, it has been pointed out that the terminal hypersurface $\mathbb{F}_4^{(1,1,2k,4k+4,6k+6)}[12k+12]$ can also be viewed as an elliptic fibration over the Hirzebruch surface \mathbb{F}_{2k} [35]. As we will explain shortly, in this setting it is natural to consider $k = 0$ as well as $k = \text{half-integer}$. We will end this section with a few comments on the latter situation.

When $k = 1/2$, the second E_7 can be broken completely so that $G_2^{(0)}(1/2) = SU(1)$. When $k = 3/2$, sequential breaking ends in $SU(3)$ [32]. Notice that $\tilde{v}/v = -3/2$ for a matter-free $SU(3)$. When $k = 5/2$ the breaking can proceed to $G_2^{(0)}(5/2) = F_4[42]$. For a matter-free F_4 , $\tilde{v}/v = -5/2$ [39], as expected. When $k = 7/2$, there is no known breaking, the terminal group is just E_7 with a half **56** hypermultiplet. Finally, the values $k = 9/2, 11/2$ require $n_T = 4, 2$ tensor multiplets and since $d_2 = 0$, the terminal group is E_8 .

3. Sequences of Reflexive Polyhedra

We now set out to study the CY spaces conjectured to give the type IIA dual description of the heterotic compactifications explained in the previous section. Our strategy is to analyze the manifolds following Batyrev's toric approach. (For a concise summary of Batyrev's construction in a form accesible to physicists see, for example, [16].) To a CY manifold (of any dimension) defined as a hypersurface in a weighted projective space one can associate its Newton polyhedron, which we denote by Δ . The Newton polyhedron is often (perhaps always) reflexive and when it is we may define the dual or polar polyhedron which we denote by ∇ . By means of a computer program we have computed the dual polyhedra for the last three manifolds given in Table 2.1. The polyhedra for each k have similar properties that we will illustrate by considering $k = 1$ as an example. For this case, the points of the dual polyhedra are displayed in Table 3.1. We shall modify these polyhedra shortly so for the present the ∇ 's are distinguished by tildes.

$4\widetilde{\nabla}SU(1)$	$4\widetilde{\nabla}SU(2)$	$4\widetilde{\nabla}SU(3)$
(-1, 0, 2, 3)	(-1, 0, 2, 3)	(-1, 0, 2, 3)
* (0, -1, 2, 3)	* (0, -1, 1, 2)	* (0, -1, 1, 1)
(0, 0, -1, 0)	(0, 0, -1, 0)	(0, 0, -1, 0)
(0, 0, 0, -1)	(0, 0, 0, -1)	(0, 0, 0, -1)
(0, 0, 0, 0)	(0, 0, 0, 0)	(0, 0, 0, 0)
(0, 0, 0, 1)	(0, 0, 0, 1)	(0, 0, 0, 1)
(0, 0, 1, 1)	(0, 0, 1, 1)	(0, 0, 1, 1)
(0, 0, 1, 2)	(0, 0, 1, 2)	(0, 0, 1, 2)
(0, 0, 2, 3)	(0, 0, 2, 3)	(0, 0, 2, 3)
(0, 1, 2, 3)	(0, 1, 2, 3)	(0, 1, 2, 3)
(1, 2, 2, 3)	(1, 2, 2, 3)	(1, 2, 2, 3)

Table 3.1: The dual polyhedra for $k = 1$ and $r = 1, 2, 3$.

The following observations summarize the structure of the polyhedra:

1. For each polyhedron all the points except two (the first and the last) lie in the hyperplane $x_1 = 0$. In each case the points that lie in the hyperplane $x_1 = 0$ themselves form a reflexive polyhedron which is the dual of the polyhedron for the respective $K3$ of the fibration.
2. Omitting the first two points and the last two points of each polyhedron leaves us with a two-dimensional reflexive polyhedron, ${}^2\nabla$, which is a triangle. This ${}^2\nabla$ is the dual polyhedron of the torus $\mathbb{P}_2^{(1,2,3)}[6]$, a sign of the elliptic fibration structure elucidated in ref. [35]
3. The three polyhedra of Table 3.1 differ only in the second point of each (which is distinguished by an asterisk). Let δ denote the (non-reflexive) polyhedron consisting of the common points and denote by pt_r , $r = 1, 2, 3$, the three special points $pt_1 = (0, -1, 2, 3)$, $pt_2 = (0, -1, 1, 2)$ and $pt_3 = (0, -1, 1, 1)$. Then

$${}^4\widetilde{\nabla}^{SU(r)} = \delta \cup pt_r .$$

We observe that we can add points to the polyhedra as follows without changing the Hodge numbers of the associated manifolds.

$$\begin{aligned} {}^4\nabla^{SU(1)} &= {}^4\widetilde{\nabla}^{SU(1)} \\ {}^4\nabla^{SU(2)} &= {}^4\widetilde{\nabla}^{SU(2)} \cup pt_1 \\ {}^4\nabla^{SU(3)} &= {}^4\widetilde{\nabla}^{SU(3)} \cup pt_1 \cup pt_2 \end{aligned}$$

The fact that the Hodge numbers of ${}^4\nabla^{SU(r)}$ and ${}^4\widetilde{\nabla}^{SU(r)}$ are the same may mean that the polyhedra correspond to the same manifold. However, whether this is or not the case, we will take the sequence of polyhedra on the left of these relations as defining the chain, abandoning if need be the sequence of spaces of Table 2.1 that was our original motivation.

4. The pt_r lie in the hyperplane $x_1 = 0$ and the observation above that the points of the polyhedra that lie in the hyperplane $x_1 = 0$ form a reflexive polyhedron continues to hold for the augmented polyhedra ${}^4\nabla^{SU(r)}$. We are therefore dealing with a succession of $K3$ manifolds and the relations above hold equally well if each ${}^4\nabla$ is replaced by a ${}^3\nabla$ referring to the $K3$'s.
5. Fix attention now on the polyhedra, ${}^3\nabla$, of the $K3$'s and the two dimensional polyhedron, ${}^2\nabla$, of the torus. The ${}^2\nabla$ is the same for each of the three spaces. It consists

of the 7 points that have $x_1 = x_2 = 0$. ${}^2\nabla$ divides ${}^3\nabla$ into a ‘top’, ${}^3\nabla_{\text{top}}$, consisting of points for which $x_1 = 0$ and $x_2 \geq 0$ and a ‘bottom’, ${}^3\nabla_{\text{bot}}$, consisting of points for which $x_1 = 0$ and $x_2 \leq 0$. Figure 3.1 illustrates this for the case $k = 3$ and $r = 3$. As we move up the chain ${}^3\nabla_{\text{bot}}$ changes, it is succesively

$${}^2\nabla \cup pt_1 \rightarrow {}^2\nabla \cup pt_1 \cup pt_2 \rightarrow {}^2\nabla \cup pt_1 \cup pt_2 \cup pt_3 \rightarrow \dots \quad (3.1)$$

The polyhedron ${}^3\nabla_{\text{top}}$ however is unchanged as we move up the chain.

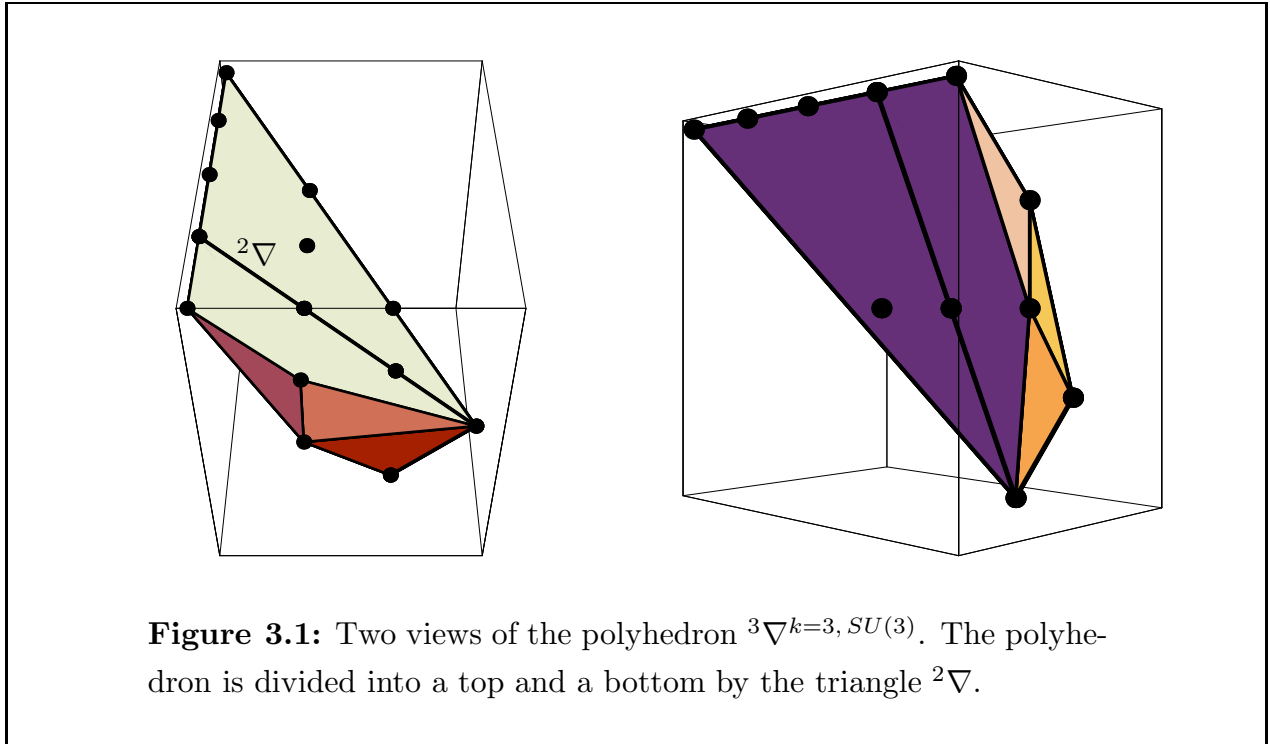


Figure 3.1: Two views of the polyhedron ${}^3\nabla^{k=3, SU(3)}$. The polyhedron is divided into a top and a bottom by the triangle ${}^2\nabla$.

We can now elaborate on our statement that for each chain a similar pattern obtains. Apart from two points, which for each member of the k 'th chain are $(-1, 0, 2, 3)$ and $(1, 2k, 2, 3)$, the points of the polyhedron lie in the plane $x_1 = 0$ forming the polyhedron, ${}^3\nabla$ of the $K3$. For each member of a chain, the polyhedron of the $K3$ is again divided into a top and a bottom by the polyhedron ${}^2\nabla$ of the torus and we may write

$${}^3\nabla^{k,H} = \nabla_{\text{top}}^k \cup \nabla_{\text{bot}}^H, \quad (3.2)$$

where ∇_{top}^k depends only on k while ∇_{bot}^H depends only on the group H that is perturbatively un-Higgsed in the heterotic side. In particular then, the dual polyhedron ${}^4\nabla^{k, SU(1)}$

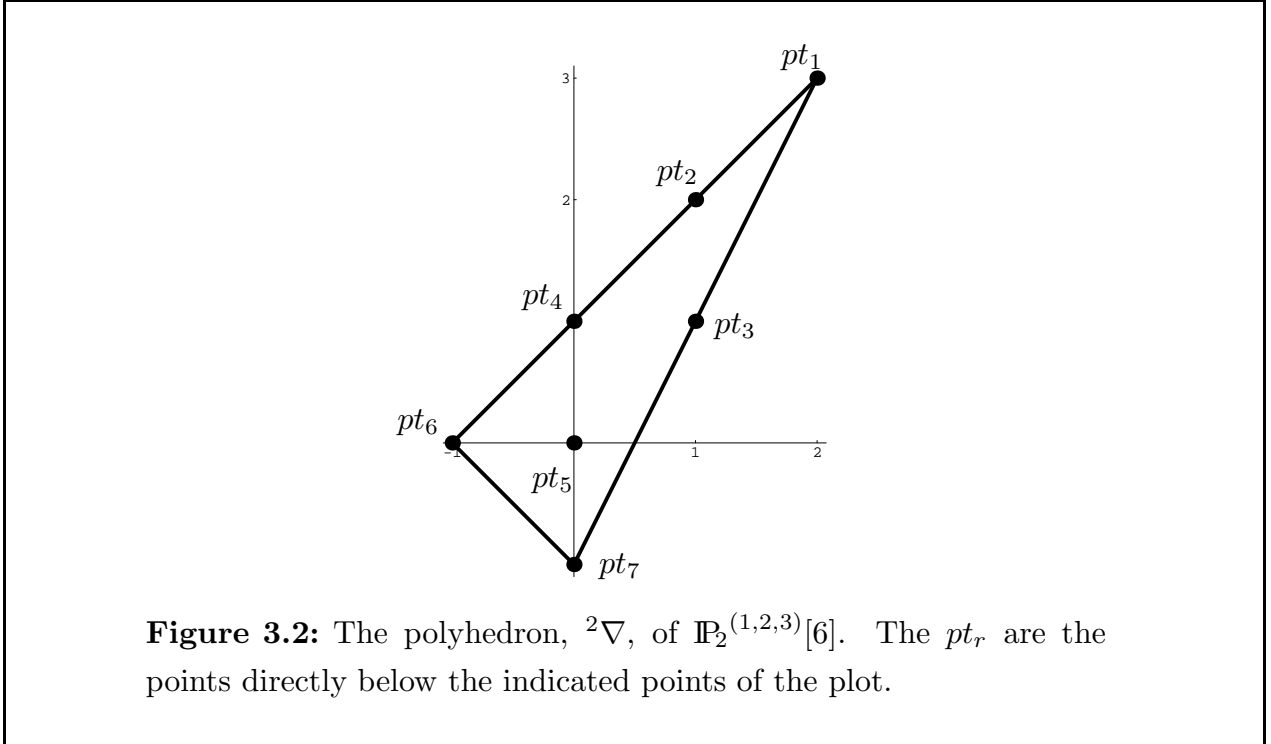
of the lowest space $\mathbb{P}_4^{(1,1,2k,4k+4,6k+6)}[12k+12]$ can be written as

$${}^4\nabla^{k,SU(1)} = {}^3\nabla^{k,SU(1)} \cup \{(-1, 0, 2, 3), (1, 2k, 2, 3)\} . \quad (3.3)$$

We can describe the tops and bottoms of ${}^3\nabla^{k,H}$ quite simply. If we denote by \mathcal{T}^k the tetrahedron with base ${}^2\nabla$ and top vertex $(0, k, 2, 3)$, the top polyhedron may be specified as follows:

$$\begin{aligned} \nabla_{\text{top}}^k &= \mathcal{T}^k , \quad \text{for } k = 1, 2, 3 \\ \nabla_{\text{top}}^4 &= \mathcal{T}^4 \cup \{(0, 1, 0, 0), (0, 2, 0, 1), (0, 3, 1, 2)\} \\ \nabla_{\text{top}}^5 &= \nabla_{\text{top}}^6 = \mathcal{T}^6 . \end{aligned}$$

The tops of the polyhedra that characterize the chains for $k = 1, 2, 3$ are shown in the Appendix.



We can also easily describe ∇_{bot}^H for $H = SU(r)$, $r = 1, 2, 3$. Consider first the polyhedron ${}^2\nabla$ shown in Figure 3.2 and let pt_r be, as previously, the points of the lattice that are directly below the corresponding points of ${}^2\nabla$. We find that

$$\nabla_{\text{bot}}^{SU(r)} = {}^2\nabla \cup \bigcup_{j=1}^r pt_j . \quad (3.4)$$

Moreover, we have verified that including the point $pt_4 = (0, -1, 0, 1)$ leads to a reflexive polyhedron that gives the expected Hodge numbers for an enhanced $SU(4)$. Further adding $pt_5 = (0, -1, 0, 0)$ corresponds to an enhanced $SU(5)$. Hence, eq. (3.4) is actually valid for $r = 1, \dots, 5$. The $\nabla_{\text{bot}}^{SU(r)}$ are shown in the Appendix. Note that we are abandoning the $SU(4)$ manifolds of Table 2.1 in favour of the definition that we are giving here. It would be of interest to see if these manifolds are in fact the same.

k	$SU(1)$	$SU(2)$	$SU(3)$	$SU(4)$	$SU(5)$	$SU(2)^2$	$SU(2)^3$
0	(243, 3)	(214, 4)	(197, 5)	(182, 6)	(167, 7)	(185, 5)	(156, 6)
$\frac{1}{2}$	(243, 3)	(202, 4)	(179, 5)	(160, 6)	(142, 7)	(165, 5)	(132, 6)
1	(243, 3)	(190, 4)	(161, 5)	(138, 6)	(117, 7)	(145, 5)	(108, 6)
$\frac{3}{2}$	(251, 5)	(186, 6)	(151, 7)	(124, 8)	(100, 9)	(133, 7)	(92, 8)
2	(271, 7)	(194, 8)	(153, 9)	(122, 10)	(95, 11)	(133, 9)	(88, 10)
$\frac{5}{2}$	(295, 7)	(206, 8)	(159, 9)	(124, 10)	(94, 11)	(137, 9)	(88, 10)
3	(321, 9)	(220, 10)	(167, 11)	(128, 12)	(95, 13)	(143, 11)	(90, 12)
$\frac{7}{2}$	(348, 10)	(235, 11)	(176, 12)	(133, 13)	(97, 14)	(150, 12)	(93, 13)
4	(376, 10)	(251, 11)	(186, 12)	(139, 13)	(100, 14)	(158, 12)	(97, 13)
$\frac{9}{2}$	(404, 14)	(267, 15)	(196, 16)	(145, 17)	(103, 18)	(166, 16)	(101, 17)
5	(433, 13)	(284, 14)	(207, 15)	(152, 16)	(107, 17)	(175, 15)	(106, 16)
$\frac{11}{2}$	(462, 12)	(301, 13)	(218, 14)	(159, 15)	(111, 16)	(184, 14)	(111, 15)
6	(491, 11)	(318, 12)	(229, 13)	(166, 14)	(115, 15)	(193, 13)	(116, 14)

Table 3.2: The Hodge numbers (h^{21}, h^{11}) calculated from the polyhedra $\nabla^{k,H}$ for the groups $SU(1), \dots, SU(5)$, $SU(2) \times SU(2)$ and $SU(2) \times SU(2) \times SU(2)$.

We have also explored the obvious possibility of adding subsets of the pt_r or other extra points to determine whether the resulting polyhedron is reflexive and whether the

Hodge numbers can be interpreted as un-Higgsing in the heterotic picture. We find that this is the case, for example, for the subsets $\{pt_1, pt_2, pt_4\}$ and $\{pt_1, pt_2, pt_4, pt_6\}$. The un-Higgsed group can be identified, in these cases, as $[SU(2)]^2$ and $[SU(2)]^3$. Hence, in symbols,

$$\begin{aligned}\nabla_{\text{bot}}^{[SU(2)]^2} &= {}^2\nabla \cup pt_1 \cup pt_2 \cup pt_4 \\ \nabla_{\text{bot}}^{[SU(2)]^3} &= {}^2\nabla \cup pt_1 \cup pt_2 \cup pt_4 \cup pt_6 .\end{aligned}\tag{3.5}$$

The Hodge numbers recorded in Table 3.2 can be seen to agree with eq. (2.10).

We wish to consider also the cases for which $k = 0$ and $k = \text{half-integer}$. It is simplest to discuss first the cases $k = \frac{3}{2}, \frac{5}{2}, \dots, \frac{11}{2}$. For these cases the manifolds in the left hand column of Table 2.1 still make sense though the $K3$ -fibration is less easy to see. On constructing the duals of the Newton polyhedra we find that precisely the same structure emerges as for the case of k integral. In particular all points except two lie in a plane and these points form the polyhedron, ${}^3\nabla$, of a $K3$. This shows that the manifolds are indeed $K3$ -fibrations with generic fibre corresponding to the polyhedron ${}^3\nabla$. Again each ${}^3\nabla$ contains a ${}^2\nabla$ which divides the ${}^3\nabla$'s into tops and bottoms with the bottoms independent of k .

For $k = 0$ the manifolds of Table 2.1 make no sense since the weight of the third coordinate would be zero. While for $k = \frac{1}{2}$ the lowest member of the chain would be $\mathbb{P}_4^{(1,1,1,6,9)}$ [18] which is not a $K3$ -fibration. The cases $k = 0$ and $k = \frac{1}{2}$ are however covered by a construction of Morrison and Vafa [35] which realizes the lowest member of each chain as an elliptic fibration over the Hirzebruch surface \mathbb{F}_{2k} . Each manifold is described as a space of seven complex variables s, t, u, v, x, y, z subject to three scaling symmetries with parameters λ, μ, ν . The variables scale with weights shown in Table 3.3.

	s	t	u	v	x	y	z	degrees
λ	1	1	$2k$	0	$4k+4$	$6k+6$	0	$12k + 12$
μ	0	0	1	1	4	6	0	12
ν	0	0	0	0	2	3	1	6

Table 3.3: The scaling weights of the elliptic fibration over \mathbb{F}_{2k} .

The Newton Polyhedron of the CY manifold defined by the data in Table 3.3 is constructed by finding all possible monomials $s^{m_1} t^{m_2} u^{m_3} v^{m_4} x^{m_5} y^{m_6} z^{m_7}$ whose degrees

under the three scalings are given by the right hand column of the Table. Owing to the three constraints on the seven exponents, m_1, \dots, m_7 , the allowed monomials lie in a four-dimensional lattice within \mathbb{R}^7 . The convex hull of the monomials is the Newton polyhedron. The polyhedron contains the point $(1, 1, 1, 1, 1, 1, 1)$, corresponding to the monomial $stuvwxyz$, as its only interior point. By translating the origin to this point, constructing the dual polyhedron and making a $GL(4, \mathbb{Z})$ transformation we obtain, in all cases, polyhedra that are exactly of the form given in (3.3). The form of the various ∇_{top}^k 's is given in Table 3.4 where the tops for all k are included for puposes of comparison. For $k = 0$ the construction yields a space that is best thought of as an elliptic fibration over $\mathbb{F}_0 = \mathbb{P}_1 \times \mathbb{P}_1$. For $k = \frac{1}{2}$ the construction yields a space that differs from $\mathbb{P}_4^{(1,1,1,6,9)}$ [18] owing to the presence of an extra constraint. In all other cases it is easy to see that this construction gives again the space $\mathbb{P}_4^{(1,1,2k,4k+4,6k+6)}$ [12k+12].

k	∇_{top}^k
$0, \frac{1}{2}, 1$	\mathcal{T}^1
$\frac{3}{2}$	$\mathcal{T}^1 \cup (0, 1, 1, 2)$
2	\mathcal{T}^2
$\frac{5}{2}, 3$	\mathcal{T}^3
$\frac{7}{2}, 4$	$\mathcal{T}^4 \cup \{(0, 1, 0, 0), (0, 2, 0, 1), (0, 3, 1, 2)\}$
$\frac{9}{2}, 5, \frac{11}{2}, 6$	\mathcal{T}^6

Table 3.4: The tops for each of the chains with $k = 0, \frac{1}{2}, \dots, 6$.

The chains themselves are constructed, as explained before, by leaving the tops alone and modifying the bottoms through the sequence (3.1). In this way we obtain Hodge numbers in accord with what we expect on the basis of the dual heterotic picture. More precisely, we find that eqs. (3.4) and (3.5) are valid for $k = 0, 1/2, \dots, 6$.

We have seen that un-Higgsing in a terminal heterotic model can be interpreted as adding points in the ${}^4\nabla_{\text{bot}}$ piece of ${}^4\nabla^k$, or equivalently, as imposing certain additional conditions on the monomial deformations that determine the dual Newton polyhedron.

Notice that in this process, the $K3$ fibers are modified. We have then a qualitative explanation of our results since, as explained by Aspinwall [10], the actual non-Abelian structure of the group that is perturbatively visible is related in turn to the structure of the $K3$ fibers.

The arguments of refs. [9, 10, 38] also provide some hints for how to look for gauge groups that cannot be seen perturbatively. The basic idea is to include the effect of degenerate fibers or to modify the \mathbb{P}_1 part of the fibration. In the dual polyhedron this can be naively mimicked by adding points outside ${}^3\nabla^{k,SU(1)}$. In fact, motivated by the shape of the polyhedron, we have noticed that adding points $(1, 2k - j, 2, 3)$, $j = 1, \dots, 2k + 2$, to ${}^4\nabla^{k,SU(1)}$ always leads to a reflexive polyhedron. Moreover, the Hodge numbers in this new sequence of polyhedra have a rather interesting pattern as we now describe.

The transitions along the new branch are characterized by

$$\Delta h_{12} = 29 \quad ; \quad \Delta h_{11} = 1 . \quad (3.6)$$

Hence, as implied by eq. (2.13), they can be explained as transitions in which $n_T \rightarrow n_T + 1$. Since, eq. (2.12) requires $(d_1 + d_2) \rightarrow (d_1 + d_2 - 1)$, this corresponds to shrinking of an instanton [32, 33]. The new sequence of polyhedra has then a non-perturbative interpretation. The observed transitions are dual to some heterotic dynamics that can only be seen in M -theory.

The result (3.6) is also compatible with un-Higgsing of a non-perturbative $SU(2)$ accompanied exactly by 16 doublets. When $k = 0$, eq. (2.5) shows that un-Higgsing of a *perturbative* $SU(2)$ precisely comes together with 16 doublets. Thus, in this case, the same group structure can appear along the perturbative and non-perturbative branches. Similar results were noticed in ref. [32] for the heterotic vacuum and in ref. [38] for the type II vacuum. In our approach this is manifest given the \mathbb{Z}_2 symmetry $x_1 \leftrightarrow x_2$ of the $k = 0$ polyhedron (3.3) that corresponds to exchange of the \mathbb{P}_1 's in $\mathbb{F}_0 = \mathbb{P}_1 \times \mathbb{P}_1$. Thus, adding points pt'_i obtained from pt_i by $x_1 \leftrightarrow x_2$ leads to the same perturbative groups but with a non-perturbative interpretation since we have left fixed the original $K3$ generic fiber.

4. Conclusions

In this article we have considered $K3 \times T^2$, $E_8 \times E_8$ compactifications with instanton numbers (d_1, d_2) and n_T tensor multiplets. Matching of spectra [1,8], and arguments based on F -theory [36,35], indicate that at the points of maximal symmetry breaking heterotic theories of this type are dual to type IIA compactifications on Calabi–Yau manifolds that admit a $K3$ as well as an elliptic fibration. The new contribution here is the observation that sequences of reflexive polyhedra associated to these spaces are nested in such a way as to reflect heterotic perturbative and non-perturbative processes. This qualitative observation is supported by quantitative agreement of the computed Hodge numbers and the number of tensor, vector and hypermultiplets in the heterotic side.

A comment concerning our results is in order. In terms of polyhedra we have only found the equivalent description of processes in which G_2 remains maximally broken while group factors $SU(r)$, $[SU(2)]^2$ and $[SU(2)]^3$ in G_1 are perturbatively restored. More complicated un-Higgsing patterns are easily envisaged and a more systematic analysis is in progress. We have certainly found other reflexive polyhedra connected, along perturbative and non-perturbative branches, to our starting models, for which we cannot provide a clear interpretation. It would be interesting to find evidence of transitions between different (d_1, d_2) that require intermediate steps in which n_T changes [33].

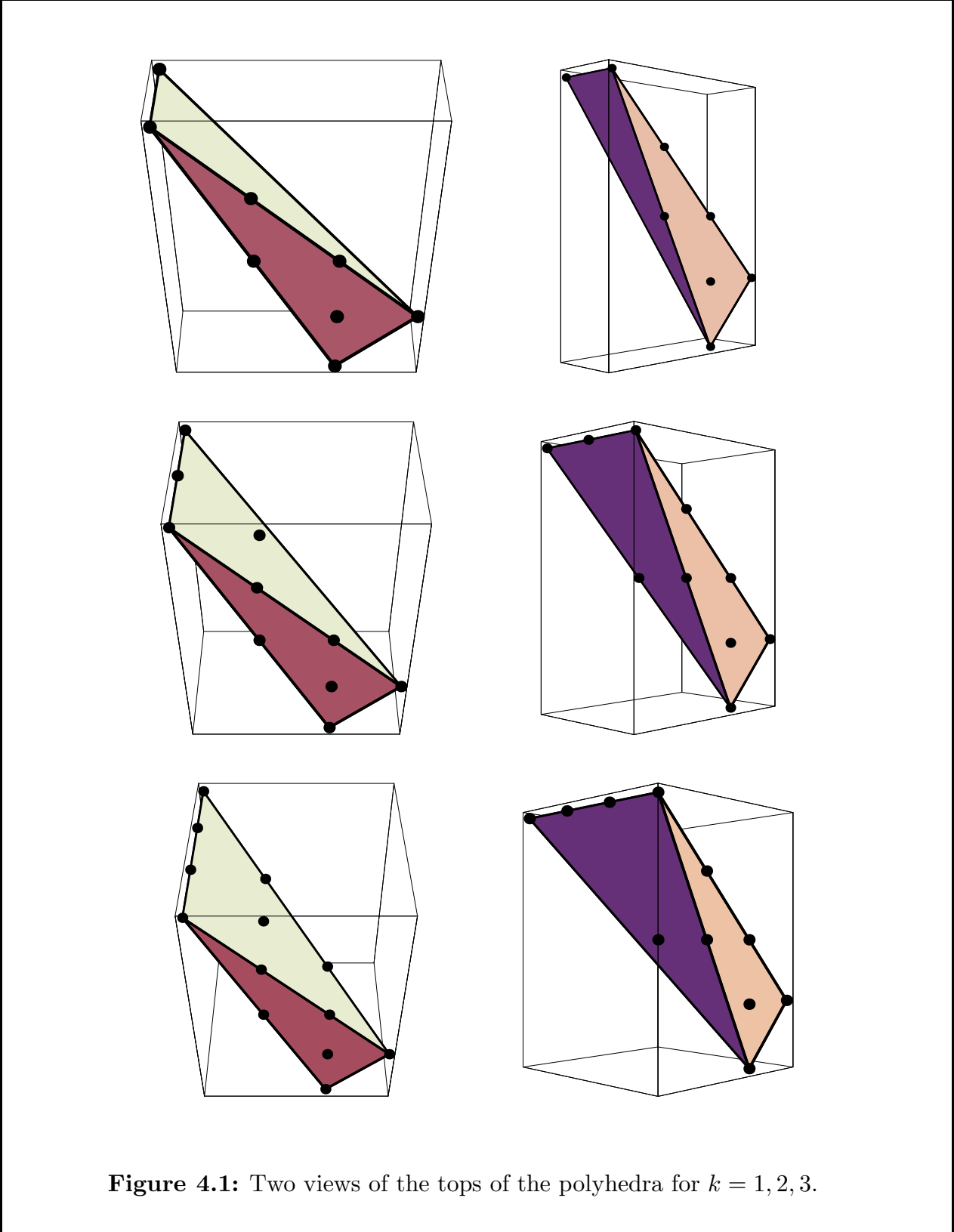
After this article was completed we received two articles[43,44] which overlap with the present work.

Acknowledgements

We had the benefit of useful conversations with G. Aldazabal, P. Aspinwall, X. de la Ossa, L. Ibáñez, V. Kaplunovsky, S. Katz, F. Quevedo and A. Uranga. This work was supported in part by the Robert A. Welch Foundation and the NSF grant PHY-9511632. A.F. acknowledges a research grant Conicit-S1-2700 and a CDCH-UCV sabbatical fellowship.

Appendix

Plots of a selection of tops and bottoms of the polyhedra are shown on the following pages.



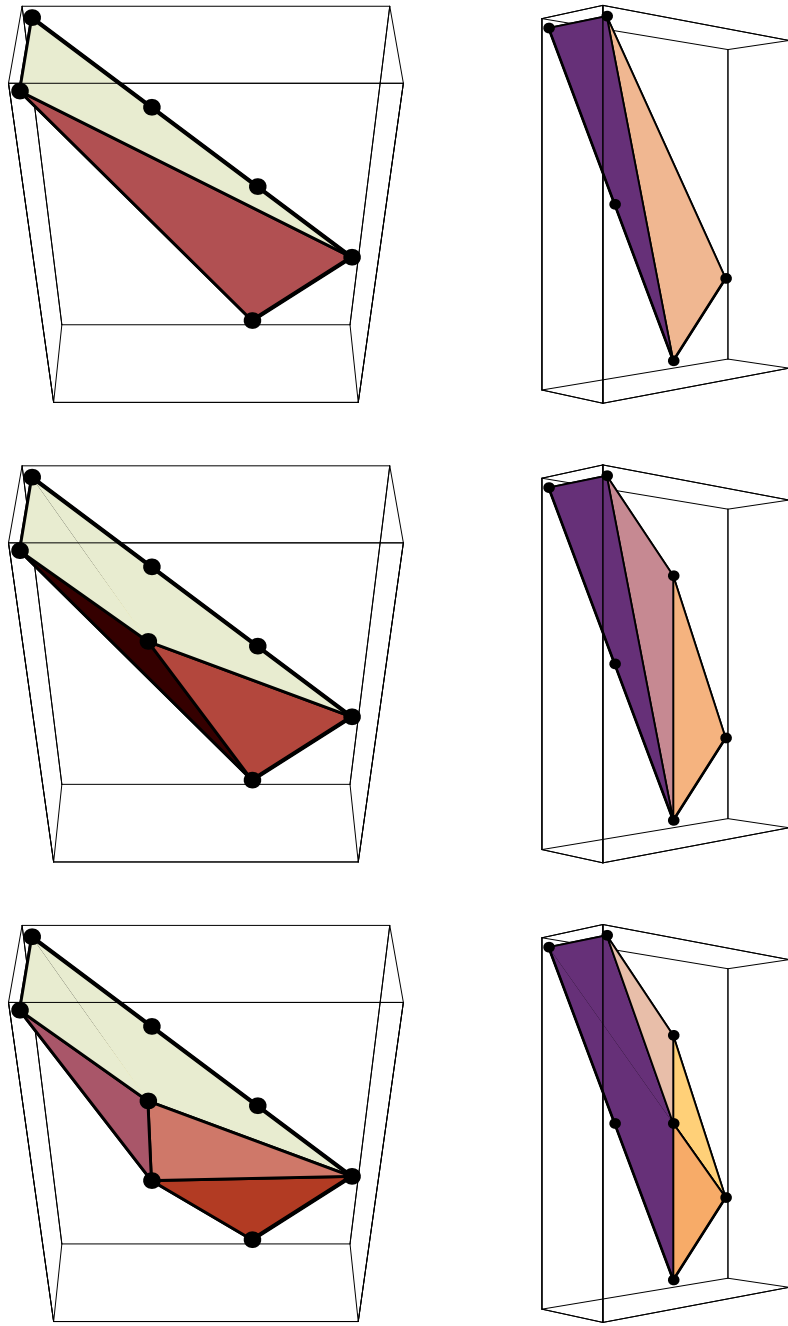


Figure 4.2: Two views of the bottoms of the polyhedra for the groups $SU(1)$, $SU(2)$ and $SU(3)$

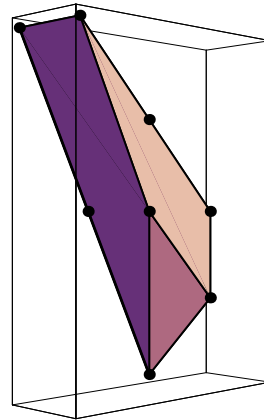
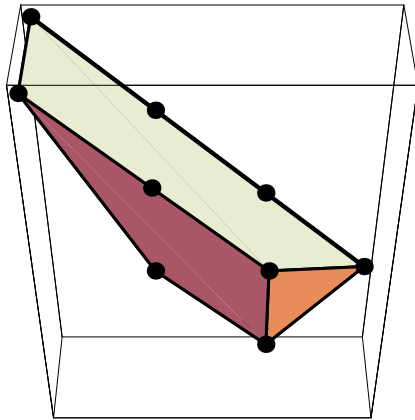
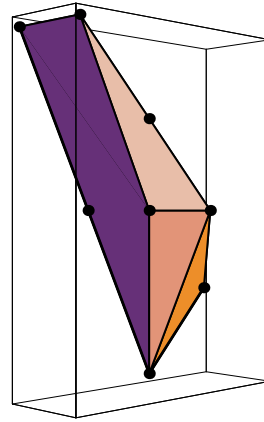
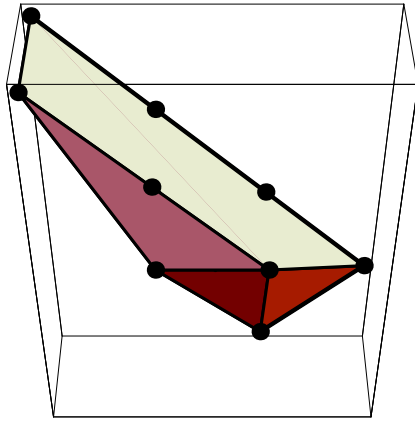


Figure 4.3: Two views of the bottoms of the polyhedra for the groups $SU(4)$, and $SU(5)$

References

1. S. Kachru and C. Vafa, Nucl. Phys. **B450** (1995) 69, hep-th/9505105.
2. S. Ferrara, J. Harvey, A. Strominger and C. Vafa, Phys. Lett. **361B** (1995) 59, hep-th/9505162.
3. A. Klemm, W. Lerche, and P. Mayr, Phys. Lett. **357B** (1995) 313, hep-th/9506112.
4. C. Vafa and E. Witten, hep-th/9507050.
5. C. Gómez and E. López, Phys. Lett. **356B** (1995) 487, hep-th/9506024;
M. Billó, A. Ceresole, R. D'Auria, S. Ferrara, P. Fré, T. Regge, P. Soriani and A. van Proyen, hep-th/9506075;
I. Antoniadis, E. Gava, K.S. Narain and T.R. Taylor, Nucl. Phys. **B455** (1995) 109, hep-th/9507115;
G. Lopes Cardoso, D. Lust and T. Mohaupt, Nucl. Phys. **B455** (1995) 131, hep-th/9507113;
G. Curio, Phys. Lett. **368B** (1996) 78, hep-th/9509146.
6. V. Kaplunovsky, J. Louis and S. Theisen, Phys. Lett. **357B** (1995) 71, hep-th/9506110.
7. S. Kachru, A. Klemm, W. Lerche, P. Mayr and C. Vafa, Nucl. Phys. **B459** (1996) 537, hep-th/9508155
8. G. Aldazabal, A. Font, L. E. Ibáñez and F. Quevedo, hep-th/9510093.
9. P. S. Aspinwall and J. Louis, Phys. Lett. **369B** (1996) 233, hep-th/9510234.
10. P. S. Aspinwall, hep-th/9511171.
11. B. Hunt and R. Schimmrigk, hep-th/9512138;
R. Blumenhagen and A. Wisskirchen, hep-th/9601050.
12. A. Klemm and P. Mayr hep-th/9601014
13. P. Berglund, S. Katz and A. Klemm, in preparation.
14. A. Klemm and R. Schimmrigk, Nucl. Phys. **B411** (1994) 559, hep-th/9204060.
15. M. Kreuzer and H. Skarke, Nucl. Phys. **B388** (1992) 113, hep-th/9205004.
16. P. Candelas, X. de la Ossa and S. Katz, Nucl. Phys. **B450** (1995) 267, hep-th/9412117.
17. H. Skarke, alg-geom/9603007.
18. V. Batyrev, Duke Math. Journ. **69** (1993) 349.

19. M. Reid, *Math. Ann.* **278** (1987) 329.
20. P. Candelas, A.M. Dale, C.A. Lütken, R. Schimmrigk, *Nucl. Phys.* **B298** (1988) 493.
21. P. Candelas, P.S. Green and T. Hübsch, *Nucl. Phys.* **B330** (1990) 49.
22. P. S. Aspinwall, B.R. Greene and D.R. Morrison, *Int. Math. Res. Notices* (1993) 319, alg-geom/9309007.
23. P. Berglund, S. Katz and A. Klemm, *Nucl. Phys.* **B456** (1995) 153, hep-th/9506091.
24. M. Lynker and R. Schimmrigk, hep-th/9511058
25. A. C. Avram, P. Candelas, D. Jančić and M. Mandelberg, hep-th/9511230
26. T.-M. Chiang, B. R. Greene, M. Gross and Y. Kanter, hep-th/9511204
27. A. Strominger, *Nucl. Phys.* **B451** (1995) 96, hep-th/9504090.
28. B. Greene, D. R. Morrison and A. Strominger, *Nucl. Phys.* **B451** (1995) 109, hep-th/9504145.
29. M. Bershadsky, V. Sadov and C. Vafa, hep-th/9510225.
30. S. Katz, D. R. Morrison and M. R. Plesser, hep-th/9601108.
31. E. Witten, *Nucl. Phys.* **B460** (1996) 541, hep-th/9511030.
32. M. Duff, R. Minasian and E. Witten, hep-th/9601036.
33. N. Seiberg and E. Witten, hep-th/9603003.
34. A. Uranga, unpublished.
35. D. Morrison and C. Vafa, hep-th/9602114.
36. C. Vafa, hep-th/9602022.
37. G. Aldazabal, A. Font, L. E. Ibáñez and F. Quevedo, hep-th/9602097.
38. P. S. Aspinwall and M. Gross, hep-th/9602118.
39. J. Erler, *J. Math. Phys.* **35** (1993) 377, hep-th/9304104.
40. P. Horava and E. Witten, *Nucl. Phys.* **B460** (1996) 506, hep-th/9510209.
41. E. Witten, hep-th/9512219.
42. V. Kaplunovsky, private communication.
43. E. Witten, hep-th/9603150
44. D. R. Morrison and C. Vafa, hep-th/9603161